

In-plane Finite Element Model of the supporting structure of an overhead contact line

0. Introduction

The aim of the work is to study the dynamic behaviour of the overhead contact line of a high-speed railway line represented in the figure below:

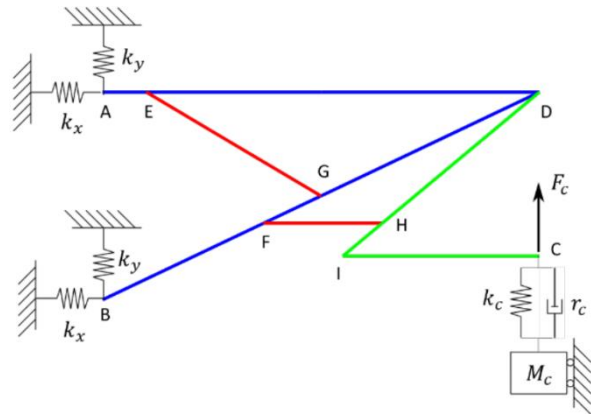


Figure 1: actual catenary (left) and its 2D model (right).

All beams are made of steel ($E = 2.06 \cdot 10^{11} \text{ N/m}^2$, $\rho = 7800 \text{ kg/m}^3$) and have tubular cross section. The structure is connected to its pole by means of springs acting in horizontal and vertical direction. A simplified way to account for the dynamic interaction with the catenary consists in a lumped mass elastically suspended in point C.

The analysis is performed exploiting a FE model, where nodes and elements are defined, and constraints are enforced.

The range of considered frequencies is 0-20 Hz.

Point	x [m]	y [m]
A	0	1.9
B (origin of reference system)	0	0
C	4	0.4
D	4	1.9
E	0.4	1.9
F	1.473	0.7
G	2	0.95
H	2.56	0.7
I	2.2	0.4

Table 1: coordinates of highlighted points.

Density [Kg/m ³]	7800
Young modulus [N/m ²]	2.06E+11
Safety coeff	1.5
Omega max [rad/s]	125.66

Table 2: mechanical and dynamical properties.

1. FE model

The input file is the file that collects all the properties of the system in terms of nodes, elements and mechanical properties.

Since the elements have to work in a quasi-static region, the maximum length must not overcome a limit value. This value depends on the highest frequency of the analysis and it can be computed using the following expression:

$$L_{max} = \sqrt{\frac{\pi^2}{\eta \Omega_{max}} \sqrt{\frac{EJ}{m}}}$$

Where Ω_{max} is the max frequency of the analysis, η is the safety factor on the maximum frequency (chosen as 1.5), m is the mass per unit length of the element and EJ is the bending stiffness. Our maximum frequency was 20 Hz. We obtain:

	Dext [mm]	Thickness [mm]	Mass [Kg/m]	J [mm ⁴]	Area [mm ²]	L max [m]
blue	60	2	2.843	153423	364.425	1.321
green	40	1.5	1.415	33666	181.427	1.077
red	25	1.5	0.864	7676	110.741	0.842

Table 3: physical and mechanical properties of the different sections.

Each beam is divided into an arbitrary number of elements, of arbitrary length each, according to the maximum length for each section type.

	Ltot	N_elements	Length [m]	Angle [rad]
AE	0.400	1	0.400	0.0000
ED	3.600	9	0.400	0.0000
BF	1.631	4	0.408	0.4435
FG	0.583	1	0.583	0.4435
GD	2.214	5	0.443	0.4435
EG	1.861	4	0.465	0.3631
FH	1.087	3	0.362	0.0000
DH	1.874	4	0.469	0.6947
HI	0.469	1	0.469	0.6947
IC	1.800	4	0.450	0.0000

Table 4: dimensions and division of the beams.

According to this division, nodes are defined, and their coordinates are computed, together with the elements which join adjacent nodes. The denomination of the elements is done according to the conventions reported in the figure.

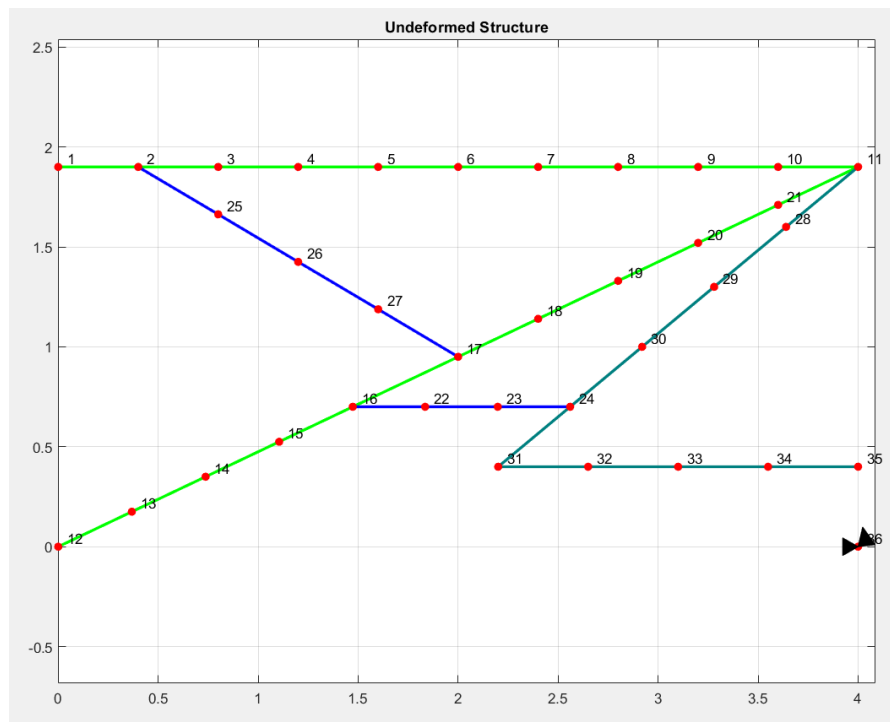


Figure 2: FE model.

NODES						
			x_c	y_c	theta_c	
AE	A	1	0	0	0	x [m]
ED	E	2	0	0	0	y [m]
		3	0	0	0	
		4	0	0	0	
		5	0	0	0	
		6	0	0	0	
		7	0	0	0	
		8	0	0	0	
		9	0	0	0	
		10	0	0	0	
	D	11	0	0	0	
BF	B	12	0	0	0	
		13	0	0	0	
		14	0	0	0	
		15	0	0	0	
	F	16	0	0	0	
FG	G	17	0	0	0	
GD		18	0	0	0	
		19	0	0	0	
		20	0	0	0	
		21	0	0	0	
FH		22	0	0	0	
		23	0	0	0	
	H	24	0	0	0	
EG		25	0	0	0	

		26	0	0	0	1.200	1.425
		27	0	0	0	1.600	1.188
DH		28	0	0	0	3.640	1.600
		29	0	0	0	3.280	1.300
		30	0	0	0	2.920	1.000
HI	I	31	0	0	0	2.200	0.400
IC		32	0	0	0	2.650	0.400
		33	0	0	0	3.100	0.400
		34	0	0	0	3.550	0.400
	C	35	0	0	0	4.000	0.400
Spring	Mass	36	1	0	1	4.000	0.000

Table 5: nodes with coordinates and degrees of constraint.

The only constrained coordinates are the horizontal displacement and the rotation of the lumped mass, since the other constraints, represented by the lumped springs, are added later in the code, directly into the stiffness matrix.

ELEMENTS				
Element	Input node	Output node	Property	Segment
1	1	2	1	AE
2	2	3	1	ED
3	3	4	1	ED
4	4	5	1	ED
5	5	6	1	ED
6	6	7	1	ED
7	7	8	1	ED
8	8	9	1	ED
9	9	10	1	ED
10	10	11	1	ED
11	12	13	1	BF
1				

31	25	26	3	EG
32	26	27	3	EG
33	27	17	3	EG
34	16	22	3	FH
35	22	23	3	FH
36	23	24	3	FH

Table 6: elements.

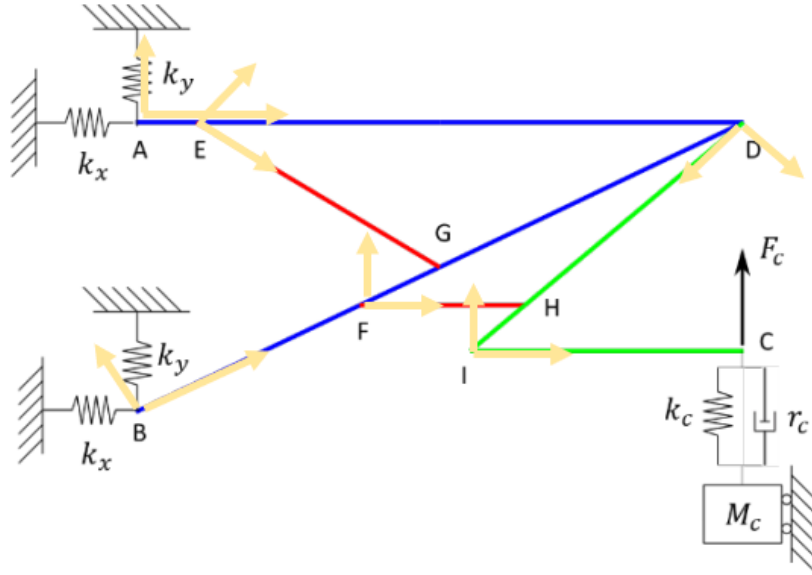


Figure 3: reference systems for the definition of each beam.

1.1 Modifications to the code

Lumped elements

The effects due to the lumped elements are added in the mass matrix, as forces per unit of acceleration, and in the stiffness matrix, as forces per unit of displacement, in correspondence of the nodes A, B and C.

% adding the springs to the ground

```
i_dof1 = idb(1,:);
```

```
i_dof12 = idb(12,:);
```

```
k = 5e4;
```

```
K(i_dof1(1),i_dof1(1)) = K(i_dof1(1),i_dof1(1)) + k ;
```

```
K(i_dof1(2),i_dof1(2)) = K(i_dof1(2),i_dof1(2)) + k ;
```

```
K(i_dof12(1),i_dof12(1)) = K(i_dof12(1),i_dof12(1)) + k ;
```

```
K(i_dof12(2),i_dof12(2)) = K(i_dof12(2),i_dof12(2)) + k ;
```

```
% concentrated mass
```

```
i_dof36y = idb(36,2) ;
```

```
Mc = 5 ;
```

```
M(i_dof36y,i_dof36y) = M(i_dof36y,i_dof36y) + Mc ;
```

```
% add kc
```

```
i_dof35y = idb(35,2) ;
```

```
i_dofkc = [i_dof35y i_dof36y] ;
```

```
kc = 1e5 ;
```

```
k_kc = [kc -kc;-kc kc] ;
```

```
K(i_dofkc,i_dofkc) = K(i_dofkc,i_dofkc) + k_kc ;
```

Damping matrix

Since the coefficients α and β are given, according to the Rayleigh hypothesis, the damping matrix is computed as:

$$[C] = \alpha[M] + \beta[K]$$

Having computed the damping matrix, it is possible to add the lumped damper.

```
% add rc
```

```
rc = 50 ;
```

```
r_rc = [rc -rc;-rc rc] ;
```

```
C(i_dofkc,i_dofkc) = C(i_dofkc,i_dofkc) + r_rc ;
```

2. Natural frequencies and mode shapes

What is done until now is the assembly of the mass matrix $[M]$ and the stiffness matrix $[K]$ by means of a pre-defined MATLAB code, then adding the contribution of the concentrated masses and springs to the obtained matrices.

At this point, natural frequencies are computed solving the eigenvalues/eigenvectors problem of the undamped system, considering the free coordinates of the system, which in our case are 106 (3 for each node minus the two constrained).

A partition of the matrices is needed in order to separate the free nodal coordinates from the constrained ones, obtaining the following matrices:

$$[M] = \begin{bmatrix} [M_{FF}] & [M_{FC}] \\ [M_{CF}] & [M_{CC}] \end{bmatrix}$$

$$[K] = \begin{bmatrix} [K_{FF}] & [K_{FC}] \\ [K_{CF}] & [K_{CC}] \end{bmatrix}$$

Natural frequencies and mode shapes are obtained by solving the following eigenvalue problem:

$$(\omega^2[I] - [M_{FF}]^{-1}[K_{FF}])\mathbf{X} = \mathbf{0}$$

The natural frequencies are the square root of the eigenvalues of the matrix $[M_{FF}]^{-1}[K_{FF}]$, while the vibration modes are the eigenvectors of the same matrix.

The first four modes and their natural frequencies are shown in the figures below, with respect to the undeformed configuration.

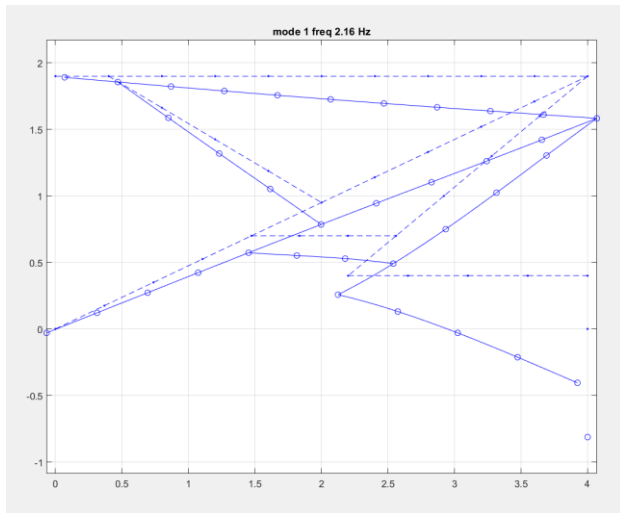


Figure 4: 1st mode shape.

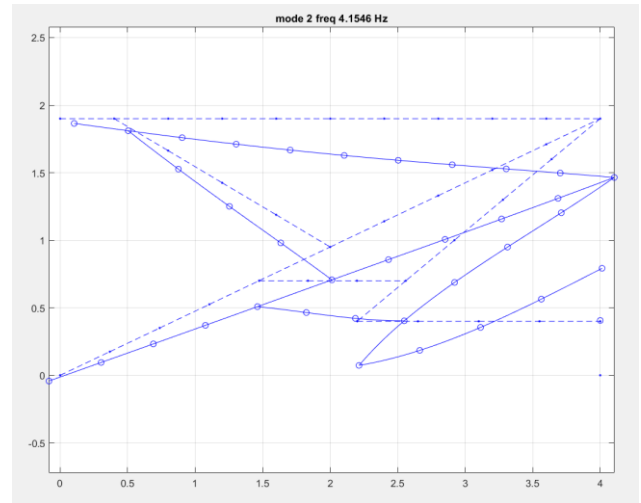


Figure 5: 2nd mode shape.

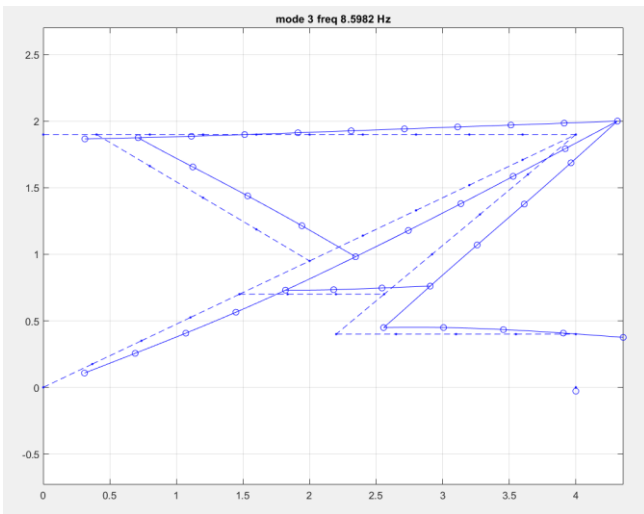


Figure 6: 3rd mode shape.

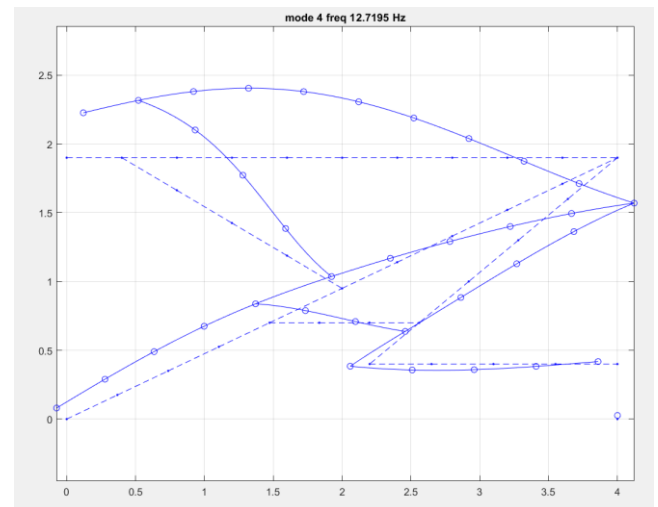


Figure 7: 4th mode shape.

3. Frequency response functions

3.1 FRF for displacements and accelerations

An harmonic force, varying in the frequency range 0-20 Hz, is applied on point C (input). The FRF is computed as the ratio between the output of the system and the input force, where the output is obtained in the considered frequency range.

Separating the free nodal coordinates from the constraint nodal ones the general equation of motion is written in the following matrix form:

$$\begin{bmatrix} M_{FF} & M_{FC} \\ M_{CF} & M_{CC} \end{bmatrix} \begin{Bmatrix} \ddot{x}_F \\ \ddot{x}_C \end{Bmatrix} + \begin{bmatrix} C_{FF} & C_{FC} \\ C_{CF} & C_{CC} \end{bmatrix} \begin{Bmatrix} \dot{x}_F \\ \dot{x}_C \end{Bmatrix} + \begin{bmatrix} K_{FF} & K_{FC} \\ K_{CF} & K_{CC} \end{bmatrix} \begin{Bmatrix} x_F \\ x_C \end{Bmatrix} = \begin{Bmatrix} F_F \\ F_C + R \end{Bmatrix}$$

And if the constraints are fixed the first equation reduces to:

$$[M_{FF}]\{\ddot{x}_F\} + [C_{FF}]\{\dot{x}_F\} + [K_{FF}]\{x_F\} = \{F_0\}e^{i\Omega t}$$

Substituting the expression of the displacement $\{x_F\} = \{X_0\}e^{i\Omega t}$ and inverting the equation we obtain:

$$\{X_0\} = (-\Omega^2[M_{FF}] + i\Omega[C_{FF}] + [K_{FF}])^{-1}\{F_0\}$$



$$\{X_0\} = [G(i\Omega)]\{F_0\}$$

In which $[G(i\Omega)] = \frac{\{X_0\}}{\{F_0\}}$ is the Frequency Response Function Matrix which gives the link between the input force and the output displacement.

The computation of horizontal displacement of point A and vertical displacement of point D is done exploiting matrix “idb”, that directly addresses to the specific node (row) and displacement (column).

Remembering that $\{x_F\} = \{X_0\}e^{i\Omega t}$ we are able to perform the time derivative of displacement in order to obtain velocity and acceleration, then for the horizontal acceleration of point A and the vertical acceleration of point D, the second derivatives of the correspondent displacements are calculated: it means that the FRF previously computed are multiplied by $-\Omega^2$, where the frequency is again the forcing frequency.

Amplitude and phase diagrams are obtained through Matlab functions “abs()” and “angle()”.

The amplitudes of the displacement are normalized with respect to the static values.

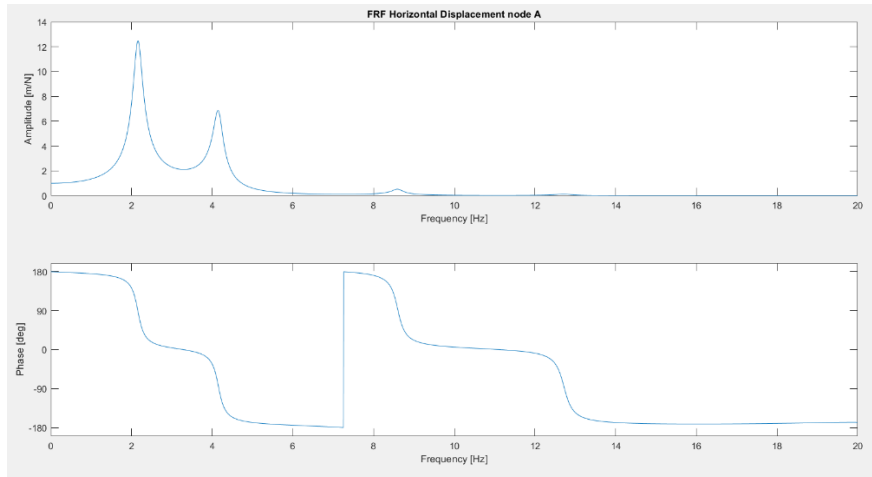


Figure 8: FRF horizontal displacement of node A, vertical force in node C. Module and phase (module normalized).

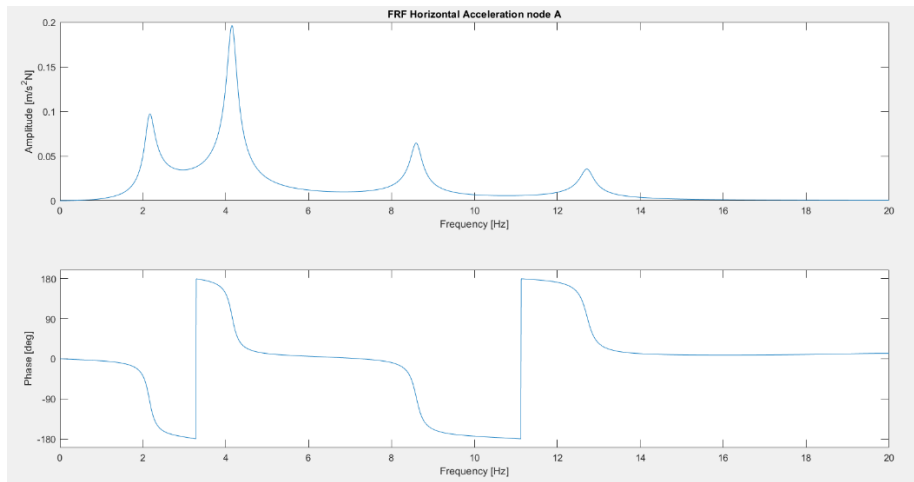


Figure 9: FRF horizontal acceleration of node A, vertical force in node C. Module and phase.

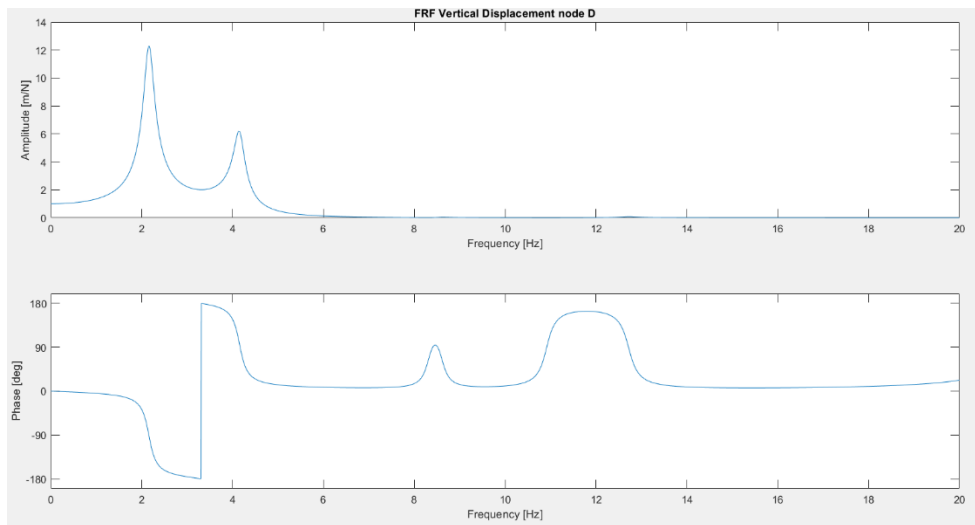


Figure 10: FRF vertical displacement of node D, vertical force in node C. Module and phase.

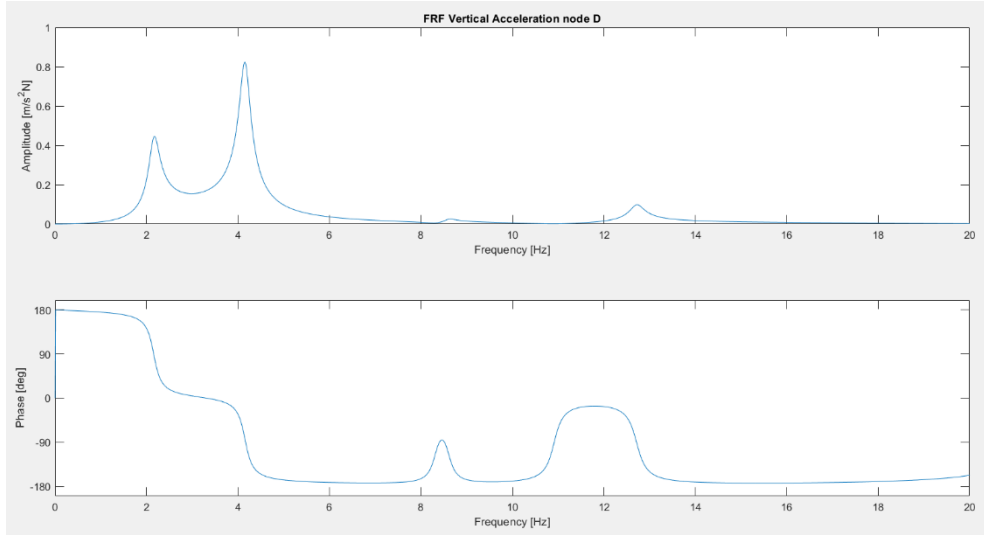


Figure 11:: FRF vertical acceleration of node D, vertical force in node C. Module and phase.

3.2 FRF for internal actions

It is then requested to calculate the internal actions in node 26 (midspan of EG element), with the variation of the forcing frequency.

According to the FE formulation, the axial and the transverse displacement of a beam section are defined as function of the nodal displacements through shape functions.

As far as axial deformation is concerned, its shape functions are assumed to be linear functions of ξ :

$$u(\xi, t) = a + b \xi$$

The axial force can be directly expressed as

$$N = \sigma A = E A \varepsilon = E A \frac{\partial u}{\partial x}$$

The axial deformation is simply defined as the ratio between the axial variation of displacements of node 26 and one of its adjacent, and the length of the element.

$$\Delta l = \frac{u_{26} - u_{25}}{l_{element}}$$

The shape functions for bending deformation are assumed to be cubic functions of ξ (beams):

$$w(\xi, t) = a + b \xi + c \xi^2 + d \xi^3$$

The bending moment and the shear force are proportional to the second and third partial derivatives of w with respect to ξ :

$$M = E J \frac{\partial^2 w}{\partial \xi^2} \quad \rightarrow \quad \frac{\partial^2 w}{\partial \xi^2} = 2c + 6d\xi$$

$$T = E J \frac{\partial^3 w}{\partial \xi^3} \quad \rightarrow \quad \frac{\partial^3 w}{\partial \xi^3} = 6d$$

From this the coefficients c and d are calculated using the local nodal coordinates of nodes 26 and its adjacent:

$$c = -\frac{3}{L^2}y_{25}^L + \frac{3}{L^2}y_{26}^L - \frac{2}{L}\vartheta_{25}^L - \frac{1}{L}\vartheta_{26}^L$$

$$d = \frac{2}{L^3}y_{25}^L - \frac{2}{L^3}y_{26}^L + \frac{1}{L^2}\vartheta_{25}^L + \frac{1}{L^2}\vartheta_{26}^L$$

Where the local coordinates are obtained multiplying the global coordinates of the nodes object of study by the rotation matrix $[\Lambda]$:

$$[\Lambda] = \begin{bmatrix} \cos(\alpha_{EG}) & \sin(\alpha_{EG}) & 0 \\ -\sin(\alpha_{EG}) & \cos(\alpha_{EG}) & 0 \\ 0 & 0 & 1 \end{bmatrix}$$

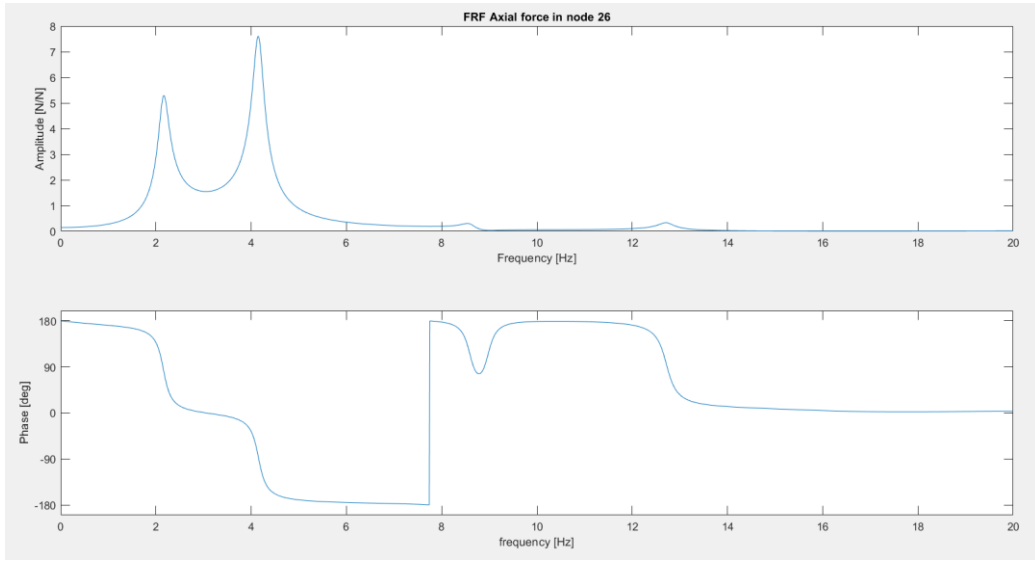


Figure 12: FRF axial force in midspan of beam EG (node 26), vertical force in node C. Module and phase.

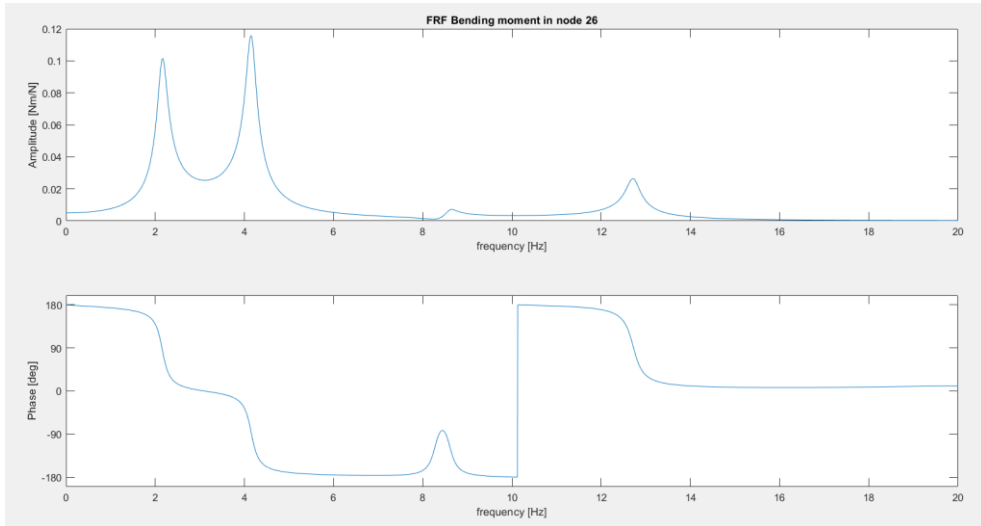


Figure 13: FRF bending moment in midspan of beam EG (node 26), vertical force in node C. Module and phase.

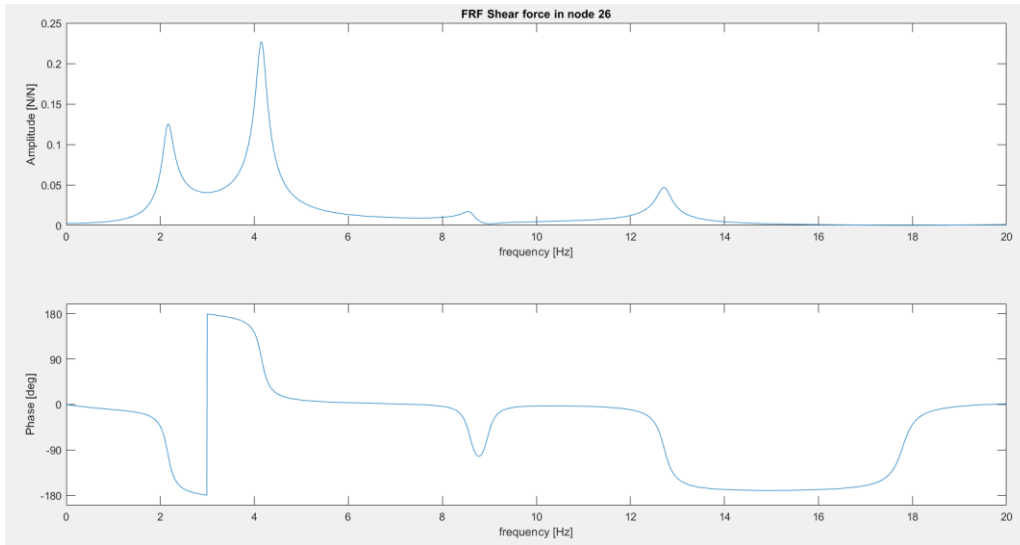


Figure 14: FRF shear force in midspan of beam EG (node 26), vertical force in node C. Module and phase.

4. Frequency response functions with modal approach

The same FRF computed before for the displacement and acceleration of nodes A and D are now computed using the modal approach, to do a comparison within the two methods.

For this purpose it's necessary to switch from the free coordinates of the NDOF system to the principal coordinates $\{q\}$, starting from the nodal displacements

$$\{x\} = [\phi]\{q\}$$

Where $[\phi]$ is the matrix of the Eigenvectors, which are obtained solving the homogeneous problem. The Eigenvectors are the shapes of the different modes of vibration and doing the operation $\{x\} = [\phi]\{q\}$ we are weighting the shapes of the different eigenvectors through the modulating new coordinates that are the principal ones.

- Mass matrix $[M_q] = [\phi]^T [M] [\phi]$
- Stiffness matrix $[K_q] = [\phi]^T [K] [\phi]$
- Damping matrix $[C_q] = [\phi]^T [C] [\phi]$
- Generalized force vector $[Q_q] = [\phi]^T \underline{F}$

The modal mass, damping, stiffness matrices and the generalized force vector are obtained through the modal matrix, which is the matrix containing the mode shapes. As an approximation only the first two modes are considered. For this reason, as we can see from the graph in the figure below, the modal approach is consistent with the result obtained with fem only in the range of frequency between 0 and 6 Hz.

The piece of code used to define matrices and force vector is here reported.

% definition of modal matrix

```
phi = modes(:,1:2) ;
```

```
% definition of modal mass,damping and stiffness matrices
```

```
Mq = phi' * MFF * phi ;
```

```
Kq = phi' * KFF * phi ;
```

```
Cq = phi' * CFF * phi ;
```

```
% generalized force vector
```

```
Qq = phi' * F0 ;
```

Our equation becomes:

$$[M_q]\{\ddot{q}\} + [C_q]\{\dot{q}\} + [K_q]\{q\} = \{Q_0\}e^{j\Omega t}$$

↓

$$\{q_0\} = \frac{\{Q_0\}}{(-\Omega^2[M_q] + j\Omega[C_q] + [K_q])}$$

Once the solution is in principal coordinates, we can go back to the free coordinates through $\{x\} = [\phi]\{q\}$.

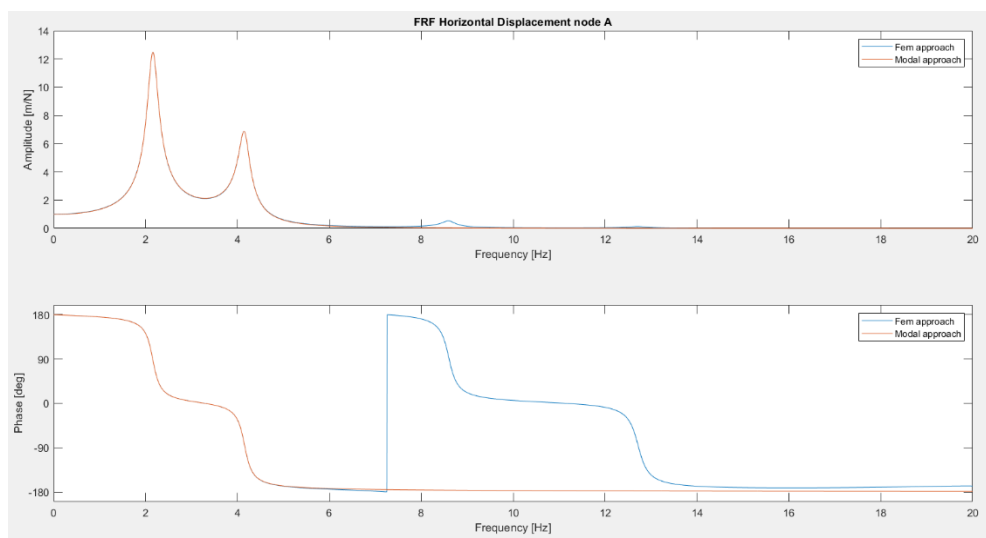


Figure 15: FRF horizontal displacement of node A, vertical force in node C. Module and phase, FEM Vs Modal approach.

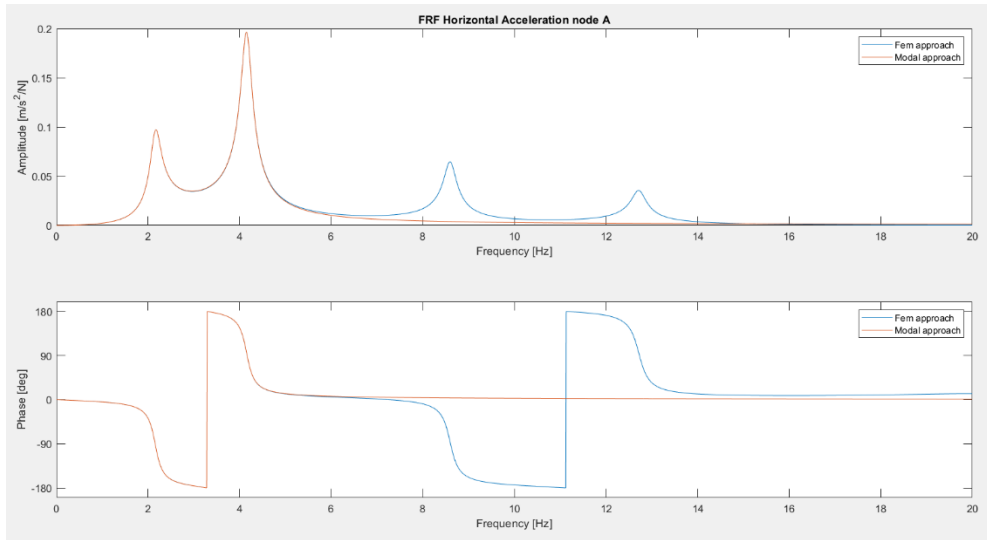


Figure 16: FRF horizontal acceleration of node A, vertical force in node C. Module and phase, FEM Vs Modal approach.

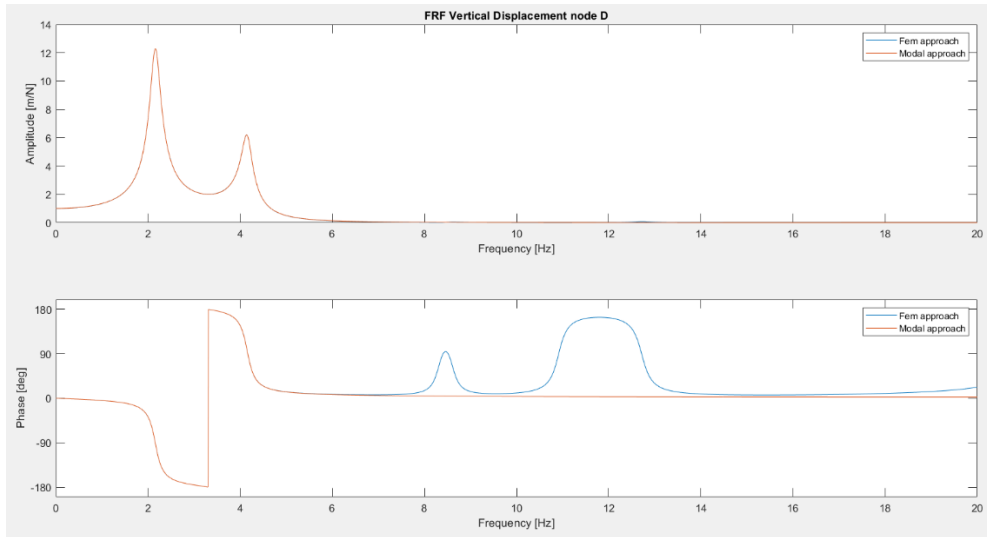


Figure 17: FRF vertical displacement of node C, vertical force in node C. Module and phase, FEM Vs Modal approach.

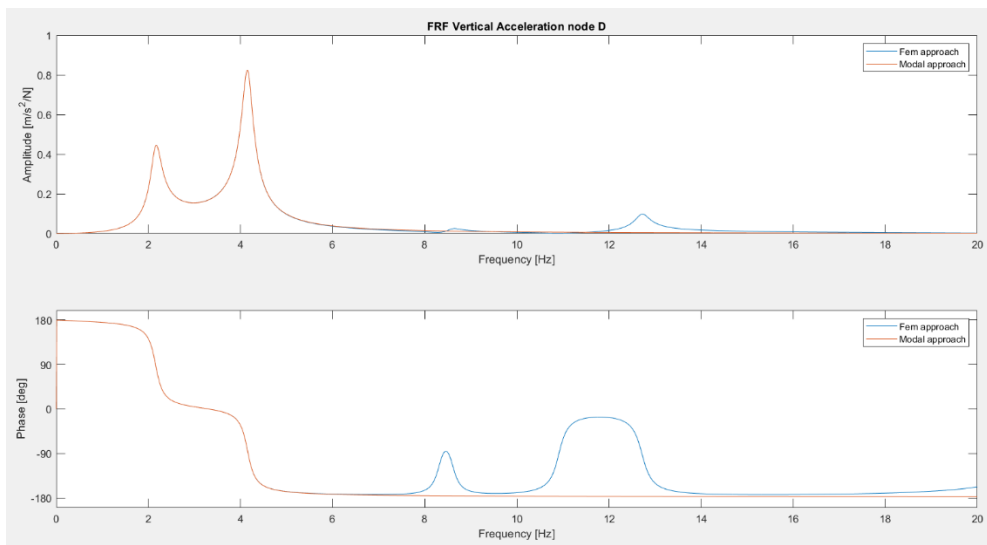


Figure 18: FRF vertical acceleration of node D, vertical force in node C. Module and phase, FEM Vs Modal approach.

In correspondence of the first resonance peaks, being the contribution of the first and second mode hugely relevant in those areas, the results are very accurate even if we considered just the first 2 modes.

Then, the presence of small differences both in amplitudes and phases can be traced back to the fact that with the modal approach we are considering just 2 vibration modes, the first and the second, not considering the entire frequency range. In fact we have to remind that the accuracy of the modal approach is higher when the number of modes taken into account increases (lower discrepancy).

5. Time history of the response

As last point it was requested to plot the time history of the vertical displacement of node D, considering a vertical force applied in node C. The force is composed by two harmonic contributions, the first one with an amplitude of 300 N and a frequency of 1 Hz, the second one with an amplitude of 50 N and a frequency of 5 Hz. The phase of both harmonic contribution is equal to zero. Since the FRF of that displacement was previously calculated, for the same force, it was possible to extract the value of the FRF for each desired frequencies and then calculate the total response summing up the result, according to the superposition principle.

```
A1 = 300 ;    %[N]   Force magnitude
A2 = 50 ;     %[N]   Force magnitude

idx1 = find (omega_vect == 1*2*pi ) ;
idx2 = find (omega_vect == 5*2*pi ) ;

time = 0 : 0.01 : 5 ;

yp1 = real(FRF_Dy(idx1)*exp(1i * omega_vect(idx1) * time) * A1) ;
yp2 = real(FRF_Dy(idx2)*exp(1i * omega_vect(idx2) * time) * A2) ;
y_tot = yp1 + yp2;
```

The plot here reported represents a time history of 5 seconds were only the particular solution is considered, thus no transitory motion is represented.

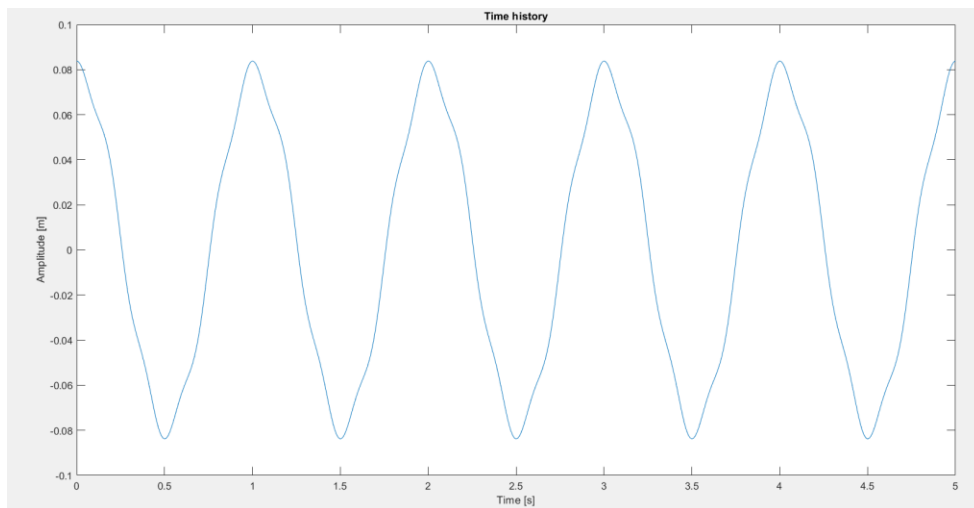


Figure 19: time history of the forced motion.